A Design Framework of Edge Phantoms for Accurate MTF Measurements at Megavoltage X-Ray Energies

Seungha Son [a], Jinwoo Kim [b], Seungjun Yoo [a], Ho Kyung Kim [a,b*]
[a]*School of Mechanical Engineering, Pusan Nat'l Univ., Busandaehakro 63beon-gil, Busan 46241*
[b]*Center for Advanced Medical Engineering Research, Pusan Nat'l Univ., Busandaehakro 63beon-gil, Busan 46241*
[*]*Corresponding author: hokyung@pusan.ac.kr*

1. Introduction

X-ray beam at kilovoltage (kV) energies is predominantly used in diagnostic radiology and industrial non-destructive testing. Some applications demand the x-ray beam with much higher megavoltage (MV) energies: for example, portal imaging in radiotherapy [1] and cargo-container screening at ports [2]. The MV image quality can be evaluated as same as done in the conventional kV images, and which consists mainly of the contrast, the noise, and the spatial resolution [3]. In the cargo inspection systems, the standard method to assess the spatial resolution is based on visual perception [4]; the minimum gap between radiopaque slabs is determined by varying the gap between the slabs. In each measurement, the slab thickness should be the same as the gap.

The modulation-transfer function (MTF) describes the contrast-transferring capability of an imaging system at each spatial-frequency content forming object to be imaged. Therefore, the MTF is known as the most objective and quantitative metric for the assessment of system spatial resolving power. To measure the MTF, the accuracy of the impulse signal is the most important. The impulse signal can be derived from a slit with a narrow gap [5] or an edge knife [6], which produces, respectively, the line-spread function (LSF) and the edge-spread function (ESF). In this study, the authors develop a design framework of the ESF at MV energies using the Monte Carlo (MC) technique.

2. Methods

2.1 Ideal ESF and MTF

For an ideal impulse signal $\delta(x, y)$, the LSF is given by

$$l(x) = \int_{-\infty}^{\infty} \delta(x, y)\, \mathrm{d}y = \delta(x), \tag{1}$$

and the corresponding MTF is evaluated as

$$\mathrm{MTF}(u) = \left| \mathcal{F}\left\{ \frac{l(x)}{\int_{-\infty}^{\infty} l(x)\, \mathrm{d}x} \right\} \right| = \frac{|T(u)|}{|T(0)|} = 1. \tag{2}$$

Therefore, if $l(x) \neq \delta(x)$, the MTF will not show a constant white spectrum. While the LSF can be directly obtained from the slit phantom, the finite extent of slit gap derives $\delta(x)$ to be blurred. Knowing this gap response, deconvolving it from the measured LSF may restore $\delta(x)$. Considering MV energies, any non-straight surface along the slit height and the imprecise slit alignment can cause additional asymmetric blurs in $\delta(x)$.

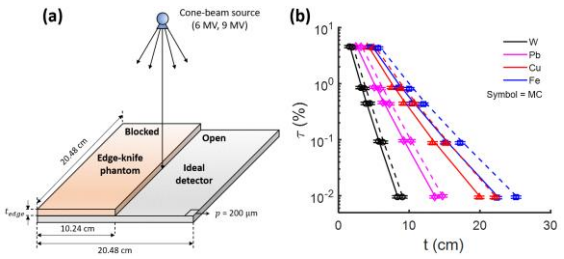

Fig. 1. (a) Simulation geometry for edge-knife measurement and (b) transmittance for the four materials. Solid and dashed lines represent 6- and 9-MV spectra, respectively.

Instead, since the relationship between ESF $e(x)$ and LSF $l(x)$ is established as

$$l(x) = \frac{\mathrm{d}e(x)}{\mathrm{d}x}, \tag{3}$$

the MTF can be readily estimated from the ESF measurement. However, the error or noise during numerical differentiation is a drawback.

2.1 Monte Carlo Framework

The mechanical design of the edge phantom is simple. However, secondary radiations produced from the edge phantom can contaminate the primary radiation-induced $\delta(x)$ [5-7]. Therefore, the main goal of the edge phantom design for the MV x-ray beam is to find materials and to determine its thickness producing secondary radiations as low as possible. The edge width L satisfying that $\int_{-L}^{L} l(x)\, \mathrm{d}x \approx 1$ is an additional design parameter [8]. This study develops an MC framework to investigate MV x-ray edge signals from various edge phantom materials with an ideal detector response.

In order to simulate the impulse response of the ideal detector for the 6- and 9-MV spectra, the MC simulations of edge-knife measurement were performed. All the MC simulations were performed using a commercial MC radiation transport code (MCNP, RSICC, Oak Ridge, TN). The particle-tracking function of the MCNP (pTrac) was used to analyze the signal spreading due to the primary and secondary interactions separately [9].

Figure 1(a) shows the simulation geometry for edge-knife measurement. A cone-beam source located at d_{SD}

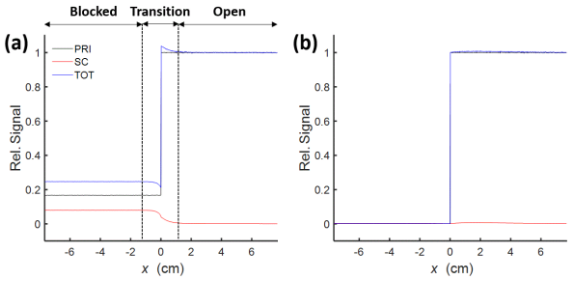

Fig. 2. ESFs obtained for the 6-MV x-ray spectrum and tungsten-edge phantom when (a) τ = 5% and (b) τ = 0.01%.

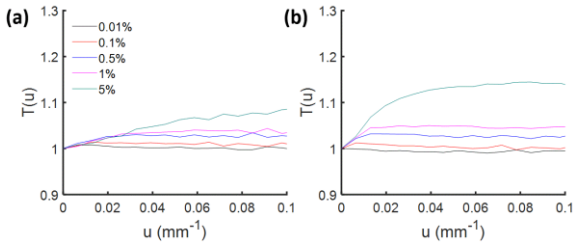

Fig. 3. MTFs obtained for the 6-MV x-ray spectrum and (a) tungsten-edge and (b) copper-edge phantoms for various τ values.

= 700 cm emits 6-MV and 9-MV x-ray spectra and the edge-knife phantom has a dimension of 10.24 × 20.48 × t_{edge} cm^3. Tungsten (W), lead (Pb), copper (Cu), and iron (Fe) are considered for absorbing materials, and the material-dependent thickness t_{edge} is determined by selecting the thickness at which the transmittance τ is 0.01, 0.1, 0.5, 1, and 5% for each material and MV spectrum $S_0(E)$. The τ was calculated by

$$\tau = \frac{\int_{-\infty}^{\infty} S_0(E) e^{-\mu(E) t_{\text{edge}}} \, \mathrm{d}E}{\int_{-\infty}^{\infty} S_0(E) \, \mathrm{d}E}. \quad (4)$$

Figure 1(b) represents τ for the four different materials and two spectra as a function of t_{edge}.

A 20.48 × 20.48 cm^2-sized ideal detector is placed in direct contact with the edge-knife phantom. The detector was modeled to completely absorb incident x-rays and do not produce any secondary photons such as fluorescent and annihilation photons. The detector has a 1,024 × 1,024 format consisting of isotropic pixels with a pitch of 0.2 mm. 2 × 10^9 photon histories were considered for each MC simulation.

The ESF was extracted from the obtained edge-knife images. The characteristics of ESFs, such as scatter-to-primary ratio, scatter fraction, undershoot, overshoot, and offset level, were quantitatively investigated in wide ranges of design parameters. To reduce the fluctuation in the MTF, the ESFs were regressed using the Gaussian-weighted moving average method. Applying Eq. (3) to the smoothed ESFs and then applying Eq. (2), the corresponding MTFs were calculated.

3. Preliminary Results

Figure 2 represents the ESFs obtained for the 6-MV spectrum and W-edge when τ is 5% and 0.01%. Since the detector is ideal to incident x-ray photons, the primary interactions show an ideal edge response while the scattered photons produced from the edge-knife phantom contaminate the signal distribution near the transition region. As shown in Fig. 2(a), the higher τ results in large undershoot and overshoot in the transition region and a large offset level in the blocked region. The former may result in the overestimation of MTF while the latter yield a zero-frequency drop in MTF.

In the case of the signal from scattered photons, the ratio of relative signals in the open and blocked regions is gradually decreased as τ increases. In particular, the signal in the open region becomes lower than that in the blocked region under high τ conditions. This can result in negative values and undershoot in the LSF.

Figure 3 shows the MTFs obtained for W- and Cu-edge phantoms using the 6-MV spectrum. As expected in Fig. 2, the MTF becomes to be overestimated as τ increases, while it shows a nearly ideal response when τ = 0.01%. Especially, Cu-edge with τ = 5% shows a significant overestimation of MTF (about 15% compared to the zero-frequency value). The material dependency may come from different scattering probabilities of W and Cu.

4. Conclusions

We have developed a framework for the design of edge-knife phantom at MV energies: MC simulations to obtain the impulse response from edge-knife phantom and the evaluation of the corresponding MTF. Depending on the phantom material, τ on the order of 5% can result in a large overestimation of MTF. The quantitative analysis of the ESF characteristics and the optimal τ values for the evaluation of the MTF will be presented at the conference.

ACKNOWLEDGEMENTS

This work was conducted as a part of the research projects of “Development of automatic screening and hybrid detection system for hazardous material detecting in port container” financially (20200611) supported by the Ministry of Oceans and Fisheries, Korea.

REFERENCES

[1] A. L. Boyer, L. Antonuk, A. Fenster, M. Van Herk, H. Meertens, P. Munro, L. E. Reinstein, and J. Wong, A Review of Electronic Portal Imaging Devices (EPIDs), Medical Physics, Vol. 19, No. 1, pp. 1-16, 1992.
[2] H. E. Martz, Jr., S. M. Glenn, J. A. Smith, C. J. Divin, and S. G. Azevedo, Poly- versus Mono-Energetic Dual-Spectrum Non-Intrusive Inspection of Cargo Containers, IEEE

Transactions on Nuclear Science, Vol. 64, No. 7, pp. 1709-1718, 2017.
[3] C. Stritt, M. Plamondon, J. Hofmann, A. Flisch, and U. Sennhauser, Performance Quantification of A Flat-Panel Imager in Industrial Mega-Voltage X-Ray Imaging Systems, Nuclear Instruments and Methods in Physics Research A, Vol. 848, No. 11, pp. 73-80, 2017.
[4] ANSI, American National Standard for Determination of the Imaging Performance of X-Ray and Gamma-Ray Systems for Cargo and Vehicle Security Screening, American National Standards Institute, ANSI N42.46-2008, 2008.
[5] A. Sawant, L. Antonuk, and Y. El-Mohri, Slit Design for Efficient and Accurate MTF Measurement at Megavoltage X-ray Energies, Medical Physics, Vol. 34, No. 5, pp. 1535-1545, 2007.
[6] K. Loot and A. Block, Accuracy of MTF Measurements with An Edge Phantom at Megavoltage X-Ray Energies, Medical Physics, Vol. 46, No. 12, pp. 5685-5689, 2019.
[7] U. Neitzel, E. Buhr, G. Hilgers, and P. R. Granfors, Determination of the Modulation Transfer Function Using the Edge Method: Influence of Scattered Radiation, Medical Physics, Vol. 31, pp. 3485-3491, 2004.
[8] S. N. Friedman and I. A. Cunningham, Normalization of the Modulation Transfer Function: The Open-Field Approach, Medical Physics, Vol. 35, pp. 4443-4449, 2008.
[9] J. Kim, H. Jeon, and H. K. Kim, Monte Carlo Dose Assessment in Dental Cone-Beam Computed Tomography, Radiation Protection Dosimetry, Vol.193, No. 3-4, pp. 190-199, 2021.